Epitaxial silicon grown on CeO_2/Si(111) structure by molecular beam epitaxy

J. T. Jones,[a] E. T. Croke,[b] C. M. Garland,[c] O. J. Marsh, and T. C. McGill
Thomas J. Watson, Sr. Laboratory of Applied Physics, California Institute of Technology, Pasadena, California 91125

(Received 23 April 1998; accepted 3 July 1998)

Using electron beam evaporation, a Si/CeO_2/Si(111) structure has been grown in a molecular beam epitaxy machine. *In situ* low energy electron diffraction, cross sectional transmission electron microscopy, selected area diffraction, and atomic force microscopy have been used to structurally characterize the overlying silicon layer and show it to be single crystalline and epitaxially oriented. Rutherford backscattering and energy dispersive x-ray analysis have been used to confirm the presence of a continuous 23 Å CeO_2 layer at the interface. Rutherford backscattering and x-ray photoemission spectroscopy show an additional presence of cerium both at the exposed silicon surface and incorporated in low levels ($\sim$1%) within the silicon film, suggesting a growth mechanism with cerium riding atop the silicon growth front leaving behind small amounts of cerium incorporated in the growing silicon crystal. © *1998 American Vacuum Society.*
[S0734-211X(98)03005-4]

I. INTRODUCTION

Cerium oxide (CeO_2) is an insulating material with a lattice mismatch of only 0.35% to silicon (Si) and an energy band gap of $\sim$5.5 eV, an attractive set of properties that could be exploited to make tunneling devices and silicon-on-insulator (SOI) structures. A significant amount of work has been done looking at the growth and characterization of CeO_2 crystals on Si by electron beam evaporation,[1–6] pulsed laser ablation,[7–10] and sputtering,[11,12] yet there have been no reports of single crystalline Si grown back on these CeO_2 films. We report here on the growth of epitaxial Si back on to a 23 Å CeO_2/Si(111) structure grown by electron beam evaporation.

II. EXPERIMENTAL DETAILS

A. Growth of CeO_2

Samples were produced from commercially available 2 in. Si(111) wafers, *n* type with 1–10 Ω cm resisitivity. After being subjected to a standard acetone, isopropyl alcohol, de-ionized water degrease in ultrasound, the wafers were etched in 50:1 HF solution until hydrophobic, rinsed in de-ionized water, and immediately introduced into vacuum. The chamber was pumped overnight and the background pressure was brought to less than 5×10^{-10} Torr in all cases. Two manually shuttered electron beam evaporators were used to deposit material from an undoped Si charge and 99.9% CeO_2 pellets to grow the structures. A reverse view low energy electron diffraction (LEED) setup allowed for *in situ* film surface characterization with a beam area of $\sim$1 mm provided the samples were first allowed to cool several hundred °C from the growth temperature. Initially, a Si buffer layer was grown by depositing 0.3 Å/s Si at 750 °C for 30 s, and then depositing a 400 Å Si film at 550 °C. Buffer layer LEED patterns were examined to assure the characteristic (7×7) reconstruction was apparent, indicative of a clean Si surface ready for further growth.

Cerium oxide thin films were grown at a wafer temperature of 550 °C, with chamber pressures ranging from 5×10^{-8} to 5×10^{-7} Torr due in part to outgassing from cerium oxide pellets, confirmed by the presence of O, CO and O_2 in residual gas analysis. To examine the effects of this background atmosphere on the clean Si surface, a test sample was run at growth conditions with the CeO_2 shutter closed and it was found that the Si crystal template remained present and acceptable for growth.

Several combinations of growth and annealing temperatures were explored in creating the thin CeO_2 films, as shown in Table I. In all cases, a CeO_2 film was grown, allowed to cool, and analyzed by *in situ* LEED. The film was then annealed and analyzed once more by LEED. A high temperature sample, CE-21, was produced with a 30 Å CeO_2 film grown at 0.3 Å/s at 750 °C which was then annealed for 10 min at 750 °C. The resulting LEED patterns both appeared amorphous. A second sample, CE-22, was produced with a 20 Å CeO_2 film grown at 0.1 Å/s at 550 °C which was then annealed for 10 min at 750 °C. The LEED showed a (1×1) pattern indicative of crystallinity, which remained but weakened upon annealing. A third sample, CE-23, was produced with a 23 Å CeO_2 film grown at 0.1 Å/s at 550 °C which was then annealed for 10 min at 750 °C. Figure 1(a) shows the resulting LEED pattern which appears amorphous both before and after anneal.

B. Growth of Si

Silicon films were then grown on two samples for which the CeO_2 was grown at 550 °C, as shown in Table I. In both cases, a thin Si film was grown and analyzed by LEED. This

[a]Electronic mail: jtj@ssdp.caltech.edu
[b]Present address: HRL Laboratories, LLC, Malibu, CA 90265.
[c]TEM facility, Materials Science Department.

TABLE I. Summary of the growth temperatures used in growing the structures. A decomposition of the CeO_2 layer was observed in CE-22, which underwent a 750 °C anneal of the Si/CeO_2/Si structure.

Sample	CeO_2 growth	CeO_2 anneal	Si growth	Si anneal
CE-21	750 °C	750 °C		
CE-22	550 °C	750 °C	550 °C	750 °C
CE-23	550 °C	750 °C	550 °C	550 °C

Si film was then subjected to an anneal and analyzed by LEED once more. Finally, the film was thickened, analyzed by LEED, and the sample was removed. For the higher temperature sample, CE-22, a 40 Å Si layer was grown at 0.3 Å/s at 550 °C which was then annealed for 10 min at 750 °C. The initial LEED patterns showed a strong (1×1) reconstruction which improved upon annealing to a (2×1) reconstruction. Lateral scanning of the sample over ~1 cm under the LEED beam resulted in no change in the LEED pattern, indicating the presence of a single crystal Si layer. The Si film was then thickened to 800 Å at 0.3 Å/s, analyzed by LEED, and removed. Upon thickening, the LEED pattern sharpened indicating improved Si crystal quality, however it will later be shown this sample underwent a thermal decomposition of the CeO_2 layer. The lower temperature sample, CE-23, had a 40 Å Si film grown at 0.3 Å/s at 550 °C which was then annealed for 10 min at 550 °C. The LEED showed a (1×1) reconstruction [Fig. 1(b)] which sharpened upon annealing [Fig. 1(c)]. The Si film was then thickened to 800 Å at 0.3 Å/s, analyzed by LEED, and removed. Upon thickening, the LEED image for CE-23 [Fig. 1(d)] began to show the characteristic (7×7) reconstruction of a clean Si(111) surface. Laterally scanning the sample under the LEED beam resulted in no change in the LEED image, again indicating the presence of a single crystal Si layer. Once removed, both CE-22 and CE-23 were cleaved into smaller pieces for further analysis.

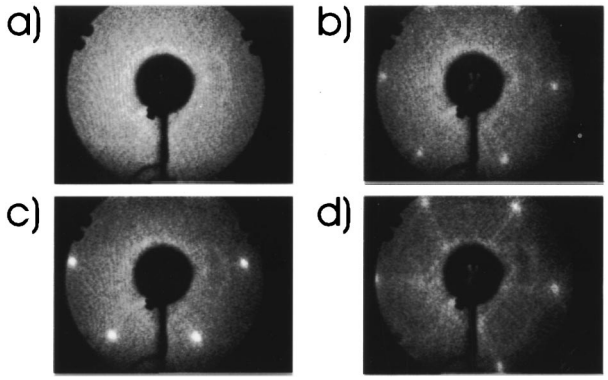

FIG. 1. *In situ* low energy electron diffraction (LEED) patterns taken at various stages of growth of CE-23. (a) After growth of 23 Å CeO_2 on Si(111), the pattern appeared amorphous. (b) Growth of 40 Å Si revealed a (1×1) surface reconstruction, which sharpened upon annealing at (c) 550 °C. (d) Thickening of the Si film to 840 Å resulted in a pattern beginning to approach a (7×7) reconstruction, indicating improved crystallinity. Lateral scanning of the LEED beam resulted in no change in the patterns, indicating single crystalline Si.

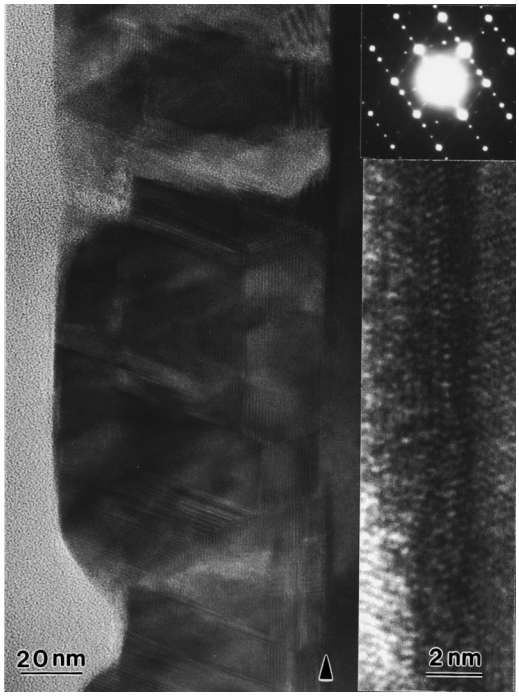

FIG. 2. Cross-sectional high resolution transmission electron microscopy of CE-23. The 23 Å CeO_2 interface (see arrow, enlargement) is shown to be continuous with no evidence of pinholes, though considerable roughness is apparent. The 840 Å Si layer (left) is shown to be epitaxial with the Si(111) substrate (right), with many instances of stacking faults and twinning along multiple (111) planes observed. Selected area diffraction (inset) with a 0.5 μm beam covering the overgrown Si layer also shows evidence of the twinning in multiple (111) planes, but the sharp spots confirm the Si layer to be single crystal.

III. RESULTS AND DISCUSSION

Transmission electron microscopy (TEM) was used to examine CE-23. Samples from the center of the wafer were prepared in cross section by standard thinning, dimpling and ion milling techniques. A Philips' EM430 transmission electron microscope was used to take high resolution transmission electron microscopy (HRTEM) images of CE-23 at 300 kV, as shown in Fig. 2. The HRTEM images reveal that the 23 Å CeO_2 interface (enlargement, Fig. 2) is continuous with no evidence of pinholes, though considerable roughness is apparent. Furthermore, the overgrown Si layer can be seen to be epitaxial with the Si(111) substrate, though somewhat defective with many instances of twinning and stacking faults. The inset of Fig. 2 shows a selected area diffraction pattern of a 0.5 μm area including the top Si layer, and while twinning along multiple (111) planes is apparent, the individual spots confirm the Si layer is single crystalline. Energy dispersive x-ray analysis (EDX) was used to confirm the presence of Ce at the interface, and no Ce was detected in the overlying Si layer.

Atomic force microscopy (AFM) was used to characterize the surface of CE-23. The film was found to have large flat regions, characterized by atomic steps spaced 100–250 nm apart, separated by pits ~50 nm across and ~20 nm deep. The source of this roughness is unclear. Figure 3 shows a 500 nm×500 nm AFM image with a vertical scale of 5 nm

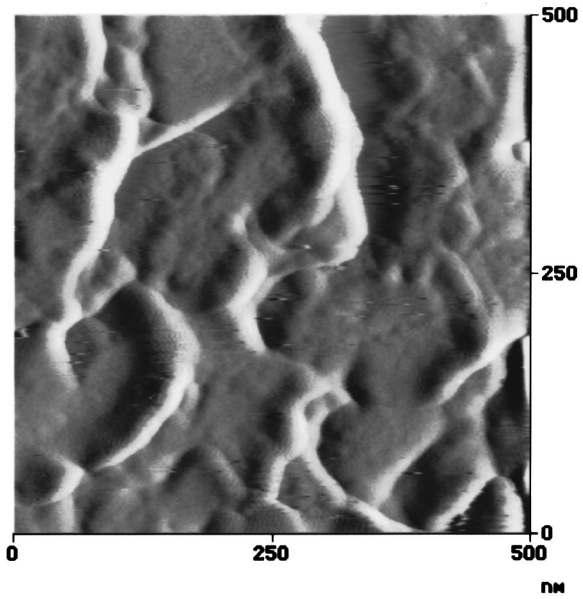

FIG. 3. Atomic force microscopy (AFM) of CE-23. This 500 nm×500 nm image with a vertical scale of 5 nm shows atomically flat regions with a rms roughness <1 nm separated by atomic steps spaced 100–250 nm apart.

FIG. 5. Cross-sectional transmission electron microscopy of CE-22 showing a thermal decomposition of the CeO_2 has taken place at 750 °C. A large cluster 50 nm across is apparent at the CeO_2 interface (see arrow). Energy dispersive x-ray analysis confirms the cluster to contain Ce, while no Ce was detected along the rest of the CeO_2 interface.

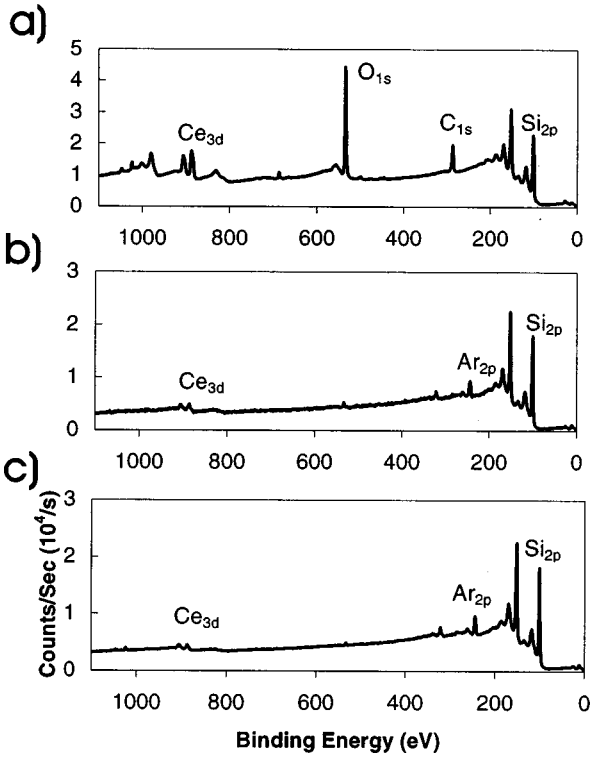

FIG. 4. X-ray photoemission spectra (XPS) taken on CE-23. By taking ratios of the Si 2*p*:Ce 3*d* peaks, adjusted for cross section, relative concentrations of Si:Ce can be found. (a) On the sample surface, the relative cerium concentration is ~2%. (b) After argon etching to remove the surface layer, the Ce concentration falls to ~1% and then (c) remains relatively constant through the Si film after up to 45 minutes of argon etching at $P_{\text{extractor}} = 10$ mPa.

in which the surface is shown to be atomically flat with a rms roughness of <1 nm in between atomic steps.

Rutherford backscattering (RBS) measurements of CE-23 were used to examine the epitaxial Si and the buried CeO_2 layer. Comparing the measured RBS curve to modeled data resulted in an excellent fit for a layer 23 Å thick and at a stoichiometric Ce:O ratio of 1:2. In addition, a second offset Ce peak was evident, indicative of Ce present at the sample surface. To further investigate the distribution of Ce throughout the overgrown Si layer, x-ray photoemission spectroscopy (XPS) was performed on CE-23 as shown in Fig. 4. As grown, a comparison of the Si 2*p*:Ce 3*d* XPS peaks yielded ~2% Ce at the surface [Fig. 4(a)], with an additional presence of oxygen and carbon from atmospheric contamination. CE-23 was then etched *in situ* at $P_{\text{extractor}}=10$ mPa with 2 kV argon ions until the oxygen signal disappeared and a second XPS scan was taken [Fig. 4(b)], yielding ~1% Ce concentration. This decrease in Ce concentration indicates there is an accumulation of Ce at the Si surface. Further argon ion etching was done for up to 45 min and XPS scans [Fig. 4(c)] reveal the Ce composition in the overgrown Si film remains relatively constant at ~1%. This distribution of Ce within the Si film is suggestive of a growth mechanism whereby excess Ce rides atop the Si growth front, leaving behind small amounts incorporated within the Si film which may be responsible for some of the previously noted defect density.

While the overlying Si film is clearly epitaxial with the Si(111) substrate, the mechanism for the growth of an epitaxial Si layer on to CeO_2 that appears amorphous by LEED

remains the focus of ongoing work. The presence of excess Ce in the as-grown Si film suggests that there may have been a surface layer of Ce atop the CeO_2 film that caused the highly surface sensitive LEED images to appear amorphous. Upon deposition of Si atop this layer, the excess Ce may ride atop the Si growth front, leaving behind crystalline CeO_2 as an epitaxial template for the growing Si. Furthermore, the rough nature of the Si/CeO_2/Si interfaces suggests that some reaction may be occurring between the Si and CeO_2 after the silicon crystal template has been passed on.

The higher temperature sample annealed at 750 °C, CE-22, was also examined by TEM at both 200 and 300 kV. The image in Fig. 5 was taken at 200 kV under two-beam conditions. Large clusters, 50 nm across, are apparent at the CeO_2 interface that were not present in the lower temperature sample images. EDX analysis shows the clusters to contain Ce, while no Ce was detected along the rest of the interface. The results support the recent report[5] of a CeO_2 thermal decomposition at 690 °C.

IV. CONCLUSIONS

In conclusion, an 840 Å Si/23 Å CeO_2/Si(111) structure has been grown. *In situ* LEED, HRTEM, and selected area diffraction confirm the overgrown Si to be both single crystalline and epitaxial with the underlying Si(111) substrate, however a large amount of twinning in multiple (111) planes is indicated. The presence of a continuous 23 Å CeO_2 film at the interface is confirmed by HRTEM, EDX, and RBS. RBS and XPS measurements show a presence of Ce at the surface of the structure, along with ~1% Ce incorporated in the Si film, suggesting a growth mechanism with Ce riding atop the Si growth front leaving small amounts behind in the growing film. HRTEM images and EDX analysis of a high temperature sample confirm the CeO_2 undergoes a decomposition during Si growth at 750 °C whereby Ce migrates to form large clusters at the interface.

ACKNOWLEDGMENTS

The authors would like to thank Robert Beach for help with the XPS and RBS measurements, and Maggie Taylor for help with the RBS measurements. This work was supported by the Defense Advanced Research Project Agency, and monitored by the Air Force Office of Scientific Research under Grant No. F49620-96-1-0021.

[1]C. Kim, K. Kim, J. Lee, K. Han, C. Park, and H. Jang, J. Korean Phys. Soc. **32**, 64 (1998).
[2]T. Inoue, Y. Yamamoto, S. Koyama, S. Suzuki, and Y. Ueda, Appl. Phys. Lett. **56**, 1332 (1990).
[3]L. Luo, X. Wu, R. Dye, R. Muenchausen, S. Foltyn, Y. Coulter, C. Maggiore, and T. Inoue, Appl. Phys. Lett. **59**, 2043 (1991).
[4]T. Inoue, Y. Yamamoto, M. Satoh, A. Ide, and S. Katsumata, Thin Solid Films **281-282**, 24 (1996).
[5]Y. Yamamoto, S. Arai, T. Matsuda, M. Satoh, and T. Inoue, Jpn. J. Appl. Phys., Part 2 **36**, L133 (1997).
[6]M. Satoh, Y. Yamamoto, and T. Inoue, Nucl. Instrum. Methods Phys. Res. B **127/128**, 166 (1997).
[7]T. Chikyow, S. Bedair, L. Tye, and N. El-Masry, Appl. Phys. Lett. **65**, 1030 (1994).
[8]L. Tye, N. El-Masry, T. Chikyow, P. McLarty, and S. Bedair, Appl. Phys. Lett. **65**, 3081 (1994).
[9]M. Yoshimoto, K. Shimozono, T. Maeda, T. Ohnishi, M. Kumaga, T. Chikyow, O. Ishiyama, M. Shinohara, and H. Koinuma, Jpn. J. Appl. Phys., Part 2 **34**, L688 (1995).
[10]A. Morshed, M. Moussa, N. El-Masry, and S. Bedair, Mater. Sci. Forum **239-241**, 291 (1997).
[11]S. Yaegashi, T. Kurihara, H. Hoshi, and H. Segawa, Jpn. J. Appl. Phys., Part 1 **33**, 270 (1994).
[12]W. Tsai and T. Tseng, J. Mater. Sci.: Mater. Electron. **8**, 313 (1997).